Effect of packing size on packed bubble column hydrodynamics

S.S. Deshpande *, J. Walker, J. Pressler, D. Hickman
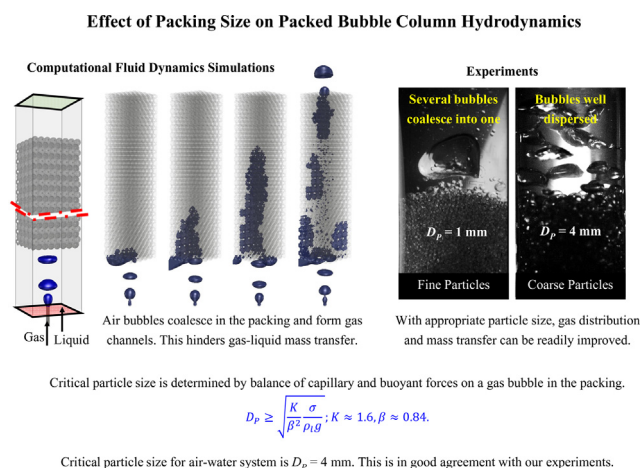
The Dow Chemical Company, Midland MI-48674, USA

HIGHLIGHTS

- Packing size strongly influences hydrodynamics in packed bubble columns.
- Depending on D_P, packing can disperse bubbles or coalesce them.
- For $D_P < 10$ mm, flow physics is dominated by balance of buoyancy & surface tension.
- Smallest D_P below which coalescence dominates is predicted using Bond number.

GRAPHICAL ABSTRACT

Effect of Packing Size on Packed Bubble Column Hydrodynamics

Computational Fluid Dynamics Simulations

Air bubbles coalesce in the packing and form gas channels. This hinders gas-liquid mass transfer.

Experiments

Several bubbles coalesce into one — $D_P = 1$ mm — Fine Particles

Bubbles well dispersed — $D_P = 4$ mm — Coarse Particles

With appropriate particle size, gas distribution and mass transfer can be readily improved.

Critical particle size is determined by balance of capillary and buoyant forces on a gas bubble in the packing.

$$D_P \geq \sqrt{\frac{K}{\beta^2} \frac{\sigma}{\rho_l g}}; K \approx 1.6, \beta \approx 0.84.$$

Critical particle size for air-water system is $D_P = 4$ mm. This is in good agreement with our experiments.

ARTICLE INFO

ABSTRACT

The present article focuses on the hydrodynamics of gas-liquid flow through a packed bubble column (PBC) reactor. Typically used in heterogeneously catalyzed gas-liquid reactions, such reactors employ a stationary packing of solid particles (catalyst) through which gas and liquid phases flow concurrently upwards. Designing the reactor to operate in a regime where the overall reaction rate is independent of mixing and mass transfer phenomena is crucial, and an important part of the design is the choice of the packing particle size, D_P. It is well known that liquid-solid mass transfer and intraparticle (void) diffusion limitations drive the choice of the largest acceptable mean particle diameter. In the present work, we provide a condition for *smallest* acceptable mean particle size based on the consideration of gas-liquid mass transfer. Using experiments in a 10" diameter PBC apparatus and computational fluid dynamics (CFD) simulations, we demonstrate that this condition is related to a balance between bubble buoyancy and surface tension and is given by $D_P > \sqrt{K\sigma/(\beta^2 \rho_l g)}$ with $K \approx 1.6$ and $\beta \approx 0.84$.

© 2018 Published by Elsevier Ltd.

1. Introduction

Heterogeneously catalyzed gas-liquid reactions are found in a number of chemical processes (Shah, 1979) such as liquid phase hydrogenation (Herrmann and Emig, 1998; Winterbottom et al., 1999) and oxidation of inorganic liquids(Komiyama and Smith, 1975). Several variants of such three phase reactors exist, such as packed bubble columns (Fan, 1989), stirred slurry reactors (Chaudhari and Ramachandran, 1980), slurry bubble columns (Schumpe et al., 1987), and trickle bed reactors (Shah, 1979). The present article focuses on hydrodynamics of packed bubble col-

Nomenclature

$A(t)$	interface area [m^2] at time t
Bo_{vl}	Bond number based on liquid flow through voids
Ca_{vl}	capillary number based on liquid flow through voids
C_e, C_i	DO concentration [mg/l] in exit and inlet streams, respectively
C^*	saturation DO concentration [mg/l] at temperature T
D_C	packing diameter [m]
D_P	particle diameter [m]
$\mathbf{e}_y$	unit vector in Y direction (0, 1, 0) [m]
$\widetilde{E}$	kinetic energy dissipation per unit liquid volume
D_v	void diameter [m]
F_B, F_C, F_I, F_μ	buoyant, capillary, inertial and viscous force scales [N]
Fr_{vl}	Froude number
g	gravitational acceleration [m/s^2]
$\mathcal{H}$	Henry's constant [Pa]
h_B	vertical coordinate of the bubble centroid [m]
H_C	packing height [m]
M_{O_2}	molar mass of oxygen gas [gram/mol]
M_{H_2O}	molar mass of water [gram/mol]
P_{O_2}	partial pressure of oxygen in the atmosphere
$\dot{Q}_g, \dot{Q}_l$	volumetric flow rates of gas and liquid, respectively [m^3/s]

Re_{vl}	Reynolds number
T	temperature [°C]
t	time [s]
$\mathbf{u}(\mathbf{x}, t)$	computational velocity field [m/s]
U_{sg}, U_{sl}	superficial velocity of gas and liquid phases, respectively [m/s]
$U_{sl,mf}$	minimum superficial liquid velocity needed for fluidization [m/s]
U_{vl}	liquid velocity through the void [m/s]
We_{vl}	Weber number
$\mathbf{x}$	spatial coordinate [m]
β	ratio of void and particle diameters [–]
Δh_B	change in vertical location of bubble centroid [m]
Δx	computational cell size [m]
$\Gamma(\mathbf{x}, t)$	liquid volume fraction in a computational cell
Λ	logarithmic concentration differential
ρ_g, ρ_l, ρ_s	gas, liquid and solid particle densities, respectively [kg/m^3]
σ	surface tension coefficient
ε	bed porosity

umns (PBC), which consists of a packing of nominally stationary solid particles (often catalysts) supported by a distributor plate. The gas and liquid phases are introduced at the bottom of the reactor and move co-currently upward, against gravity, through the packing. Depending upon the application, the packing elements could be spheres, cylinders, Raschig rings, multi-lobed elements and extrudates of various cross-sections. Here we consider only spherical particles, characterized by their diameter, D_P.

It is desirable to operate the reactor in a regime, where (i) liquid-solid mass transfer, (ii) interparticle (void) diffusion and (iii) gas-liquid mass transfer do not limit the overall reaction rate. Therefore, it is of great interest to characterize the hydrodynamics of the two phase flow through voids in the packing. The choice of particle size, D_P, affects the characteristic void size of the packing and consequently has a direct bearing on various mass transfer rates. The criteria (i) and (ii) above drive the upper limit on D_P (Shah, 1979; Weisz and Prater, 1954). The aspect of gas-liquid mass transfer, (iii), is considerably more complicated and requires a clear understanding of the hydrodynamics.

A number of researchers (Turpin and Huntington, 1967; Specchia et al., 1974; Murugesan and Sivakumar, 2002; Toukan et al., 2017) have characterized the two-phase hydrodynamics through the packing by building flow regime maps. These maps trace the effect of gas and liquid flow rates on emergence of various hydrodynamic regimes such as dispersed bubble flow, slug flow, and spray regimes. The spray regime, which occurs for very high gas flow rates and yields a gas-continuous packing with dispersed liquid droplet, is not of interest here. From the viewpoint of maximizing gas-liquid contact, operation in the dispersed bubble regime is desirable – both liquid and gas flow simultaneously through the packing. The slug flow regime, on the other hand, is often associated with maldistributed gas-liquid flow through the packing. Transition between these regimes depends in a very complicated way upon a large number parameters, including the gas and liquid flow rates, fluid properties, and properties of the particles. Consequently, each of these maps is experiment-specific and can be used reliably only over a very limited range of flow conditions. Several others (see (Alexander and Shah, 1976) for a

summary) have characterized gas-liquid and liquid-solid mass transfer coefficients, phase holdups, and pressure drop across the bed in terms of operating parameters. Note that most of these correlations are based on experiments involving relatively coarse particles – $D_P \gtrsim 3$ mm. For smaller particle sizes (<2 mm in diameter), such correlations typically do not apply (Shah, 1979; Larachi et al., 2001; Iliuta et al., 1999; Saada, 1975), which suggests that the dominant physical phenomena that drive gas-liquid contacting are different for coarse and for fine particles. The distinction between the coarse and fine particle beds is likely a reflection of the nature of hydrodynamics occurring within the interstitial volume between the particles (voids). Molga and Westerterp (1997) have found that only in the case of very coarse particles ($D_P \gtrsim 10$ mm) can a dispersed bubble regime be established, where gas bubbles and the liquid stream flow simultaneously through the voids.

Direct visualization of gas-liquid flow through the packing is desirable; however, this is not a trivial task. Only recently have researchers been able to use experiments (Motil, 2006; Chen et al. 2017; Li et al., 2016) and computations (Song et al., 2017; Boyce et al., 2017; Uzi et al., 2016; Parmigiani et al., 2011) to better understand the flow characteristics in the packing. The work of Collins et al. (2017) is of direct relevance here. The authors used magnetic resonance imaging (MRI) to visualize the motion of gas pockets in packings of monosized glass spheres ($D_P = 1.8, 3$, and 5 mm). Their visualizations revealed that the gas bubbles introduced into the PBC either moved as elongated slugs through the packing or remained attached to the packing. The key point from their work is that, as the packing particle size is reduced, the propensity for a gas pocket to remain attached to the packing increases. This is an important point, because such attachment (or slowing down) of gas pockets in the packing is at the heart of coalescence of multiple bubbles within the packing. Not surprisingly, the authors also report the presence of large gas slugs (several coalesced gas bubbles) in the case of beds of small particles ($D_P < 2$ mm). A similar observation regarding maldistribution and slug formation for particles smaller than 2 mm in diameter has also been made by Moreira and Freire (2003) as well as Lamine et al.